Plasmonics for integrated optics

Invited paper

Pierre Berini[1,2,3]
[1] *School of Electrical Engineering and Computer Science, University of Ottawa, 25 Templeton St., Ottawa, Ontario K1N 6N5, Canada, e-mail: berini@eecs.uottawa.ca*
[2] *Department of Physics, University of Ottawa, Ottawa, Ontario K1N 6N5, Canada*
[3] *Centre for Research in Photonics at the University of Ottawa, Ottawa, Ontario K1N 6N5, Canada*

ABSTRACT

We review work on integrated optical components and devices operating with surface plasmons. The properties of long-range surface plasmon waveguides are discussed, followed by their application to elements such as S-bends, Y-junction splitters, couplers and Mach-Zehnder interferometers. Such passive elements are then used to underpin advanced active devices, such as surface-plasmon amplifiers, lasers and biosensors.

Keywords: Surface plasmon waveguides, passive components, active devices, lasers, amplifiers, biosensors.

1. INTRODUCTION

Long-range surface plasmon polaritons (LRSPPs) are transverse magnetic (TM) surface waves that propagate on a thin metal slab or stripe cladded by dielectrics of similar refractive index [1]. LRSPPs can propagate up to centimeters in the infrared, which is significantly further than the propagation length of single-interface SPPs. The increased propagation length of LRSPPs is due to reduced confinement to the metal, but the increased length enables a long optical interaction between these surface waves and the surrounding claddings. LRSPPs propagating along thin narrow metal stripes are of particular interest because they are confined in the plane transverse to the direction of propagation, thereby enabling integrated optical elements as shown in Fig. 1.

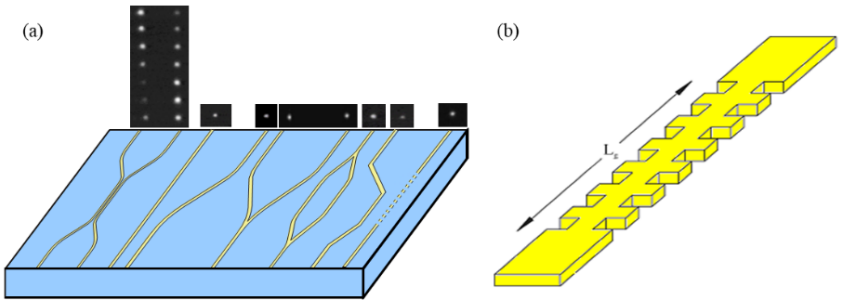

Figure 1. (a) Sketch of integrated optical elements implemented with LRSPP waveguides along with a mosaic of measured mode outputs. Left to right: edge couplers, straight segment, S-bend segment, Y-junction splitter, Mach-Zehnder interferometer (MZI), sharp bends, waveguide Bragg grating [1]. (b) Sketch of a waveguide Bragg grating implemented as a step-in-width metal stripe structure.

Integrated optical elements based on LRSPPs have compelling performance characteristics and are easy to fabricate. Many of the required elements have been fabricated and demonstrated experimentally, and are used in applications. Fig. 1(a) summarises some of the elements of interest, including parallel waveguide couplers, a straight waveguide, S-bend, Y-junction splitter, single-output Mach-Zehnder interferometer (MZI), sharp bends, and a waveguide Bragg grating. The latter is typically implemented as a step-in-width metal stripe structure, as sketched in Fig. 1(b). Mode outputs from typical structures captured using an infrared camera are also shown in Fig. 1(a); the structures were fabricated as thin (20 nm) Au stripes on SiO_2 and covered by an index-matched medium [1]. Low attenuation values of a few dB/mm are routinely achievable in the infrared (*e.g.*, λ_0 ~ 1310 and 1550 nm) along with near-perfect end-fire coupling (>90% efficiency) to dielectric waveguides and optical fibre.

2. ACTIVE PLASMONIC DEVICES

Significant theoretical and experimental work has been conducted over the past decade to compensate for surface plasmon loss or even produce amplification and lasing with surface plasmons [2]. Lasing with surface plasmons is of strong current interest because the structures can be miniaturized, offering compact coherent sources for integrated photonic or plasmonic circuits [3,4]. LRSPPs with their low attenuation are attractive for active plasmonic applications because many active materials have sufficient gain to overcome the losses so demonstrations and proof-of-principle studies are readily undertaken. Also, LRSPP amplifiers and lasers can be integrated with passive elements (*e.g.*, Fig. 1) to enable advanced functionality circuits.

One of the first demonstrations of surface plasmon amplification was carried out using LRSPPs on a thin Au stripe on SiO_2, cladded by an optically-pumped dipolar gain medium (IR-140 dye molecules in solvent), where a modal gain of about 10 dB/mm was measured [5]. Work was also carried out to incorporate the same dye molecules (IR-140) into PMMA to produce a solid-state gain medium that could be readily spin-coated onto substrates, integrated with other materials, and structured using e-beam litho [6,7]. Optimisation of the medium led to optically-pumped gain of 80 to 300 cm^{-1} at 880 nm [7]. The medium can provide long-term (low-bleaching) gain as long as the pump repetition period is greater that the thermal characteristic time of the medium. The medium structured by e-beam litho retains much of its gain as long as the dose is not too high [7].

LRSPP laser concepts were proposed theoretically and the requirements for single-mode lasing investigated [8]. LRSPP distributed feedback (DFB) lasers were then realized and demonstrated [9], as summarised in Fig. 2. The lasers consist of a 20 nm thick Au stripe on a thick silica layer, covered with 600 nm of PMMA doped with IR-140 as the active medium. The Au stripe was stepped in width in a pitch of $\Lambda \sim 300$ nm (*cf.* Fig. 1(b)), forming a Bragg grating with a centre wavelength of $\lambda_B \sim 880$ nm, corresponding to the peak emission wavelength of IR-140 dye molecules. The laser was pumped from the top and the emission emerged from a facet, as shown in Fig. 2(a). Fig. 2(b) shows the measured peak emission intensity *vs.* pump power density for such a laser, from which a clear lasing threshold is identified (I_p = 1.04 MW/cm^2). Fig. 2(c) shows the evolution of the output spectrum beyond threshold as the pump power density is increased, revealing lasing in a single mode and significant linewidth narrowing (the spectrum measured for I_p = 2.88 MW/cm^2 is spectrograph-limited). The inset to Fig. 2(b) shows an output mode beyond threshold captured on an IR camera. DFB lasers such as this are compact and easy to fabricate and integrate with other optical elements (*cf.* Fig. 1(a)).

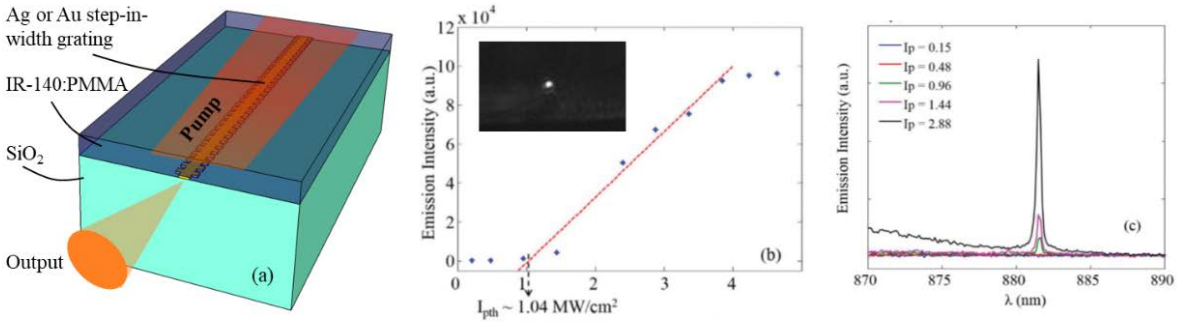

Figure 2. (a) Sketch an LRSPP DFB waveguide laser. (b) Measured peak emission intensity vs. pump power density (MW/cm^2) for a Au DFB laser; the lasing threshold is 1.04 MW/cm^2 [9]. (c) Linewidth narrowing with increasing pump power density (Ip in MW/cm^2) [9].

3. BIOSENSORS

LRSPPs on metal stripe waveguides are attractive for biosensing applications because an integrated optical geometry (*cf.* Fig. 1) can be used as a transducer, and the low attenuation enables a long interaction length with the sensing medium. Furthermore, the biosensors are compact and mass manufacturable using semiconductor fabrication tools and processes. An LRPP waveguide biosensor is shown Fig. 3(a), which illustrates a Au stripe on Cytop within a fluidic channel filled with sensing solution [10]. The thin red region models a biochemical adlayer forming on the metal stripe during sensing. The LRSPP propagates over a broad range of wavelengths with the field distribution shown in Fig. 3(b). This field distribution is symmetric-like, leading to efficient butt-coupling to a TM-polarised optical fibre or beam. Fig. 3(c) shows a SEM of fabricated structures and Figs. 3(d)-(e) fluidic fixturing and interfacing. Figs. 3(f)-(h) show single-output [11], dual-output [12] and triple-output [13] (MZIs), where one of the arms is exposed to the sensing fluid via a microfluidic channel of length L_F. LRSPP waveguide biosensors were used successfully for disease detection in complex fluids [14], including Dengue infection in patient blood plasma [15], leukemia in patient blood sera [16], and bacteria in urine [14].

Sensing occurs as biomaterial binds selectively to the top surface of the stripe functionalised with appropriate recognition chemistry - *e.g.*, antigen immobilised on the waveguide to capture antibodies in a patient sample. As binding occurs, a biochemical adlayer forms on the surface of the stripe (red region, Fig. 3(a)), which perturbs the propagation of the LRSPP, leading to changes in its intensity and phase. Both changes can be measured in real time, the former via a straight waveguide and the latter via a MZI (Figs. 3(f)-(h)). Single-output MZIs (Fig. 3(f)) are simpler, but multiple-output MZIs provide advantages: Dual-output MZIs (Fig. 3(g)) provide twice the dynamic range (twice the sensitivity) when operated in differential mode, as shown in Fig. 3(i), and the ability to suppress the effects of common perturbations and drift by referencing to the sum of the outputs. Similarly, triple-output MZIs suppress common perturbations and increase the dynamic range, but additionally they mitigate sensitivity fading and resolve directional ambiguity when unwrapping the phase.

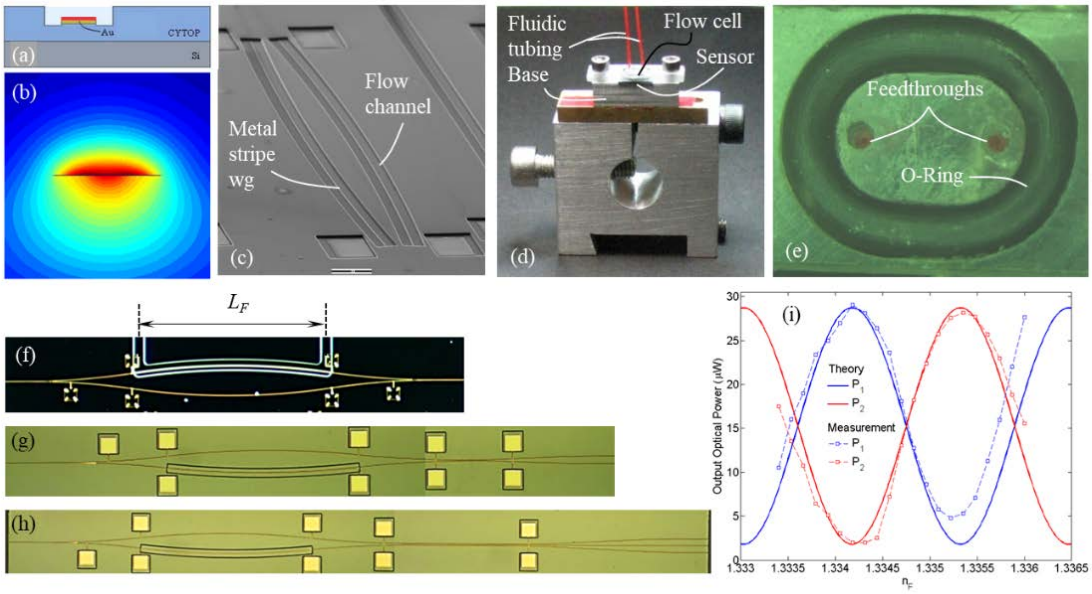

Figure 3. (a) Cross-sectional sketch of an LRSPP waveguide biosensor, (b) LRSPP field distribution, (c) SEM image of biosensors, (d) fixture housing a biosensor, (e) flow cell lid. Microscope images of (f) single-output [11], (g) dual-output [12] and (h) triple-output [13] MZI biosensors, with a microfluidic channel of length L_F. (i) Measured and theoretical responses of a dual-output MZI biosensor [12].

4. CONCLUSIONS

Integrated optics using LRSPPs on metal stripe waveguides is compelling. The low attenuation of LRSPPs enables a long optical interaction length with the claddings as well as amplification using conventional gain materials. The technology is promising for several applications, including amplification, lasing and biosensing.

REFERENCES

[1] Berini, P., "Long-range surface plasmon polaritons," *Adv. Opt. Phot.* 1, 484-588 (2009).
[2] Berini, P. and De Leon, I., "Surface plasmon-polariton amplifiers and lasers," *Nat. Phot.* 6, 16-24 (2012).
[3] Bergman D. J. and Stockman, M. I., "Surface Plasmon amplification by stimulated emission of radiation: Quantum generation of coherent surface plasmons in nanosystems," *Phys. Rev. Lett.* 90, 027402 (2003).
[4] Ma, R. M., Oulton, R. F., Sorger, V. J., Bartal, G., and Zhang, X., "Room-temperature subdiffraction-limited plasmon laser by total internal reflection," *Nat. Mat.* 10, 110-113 (2011).
[5] De Leon, I., and Berini, P., Amplification of long-range surface plasmons by a dipolar gain medium. *Nat. Phot.* 4, 382-387 (2010).
[6] Hahn, C., Song, S. H., Oh, C. H., and Berini, P., "Plasmonic gain in long-range surface plasmon polariton waveguides bounded symmetrically by dye-doped polymer," *Appl. Phys. Lett.* 107, 121107 (2015).
[7] Amyot-Bourgeois, M. *et al.*, "Gain optimization, bleaching and e-beam structuring of IR-140 doped PMMA, and integration with plasmonic waveguides," *Opt. Mat. Exp.* 7, 3963-3978 (2017).
[8] Karami Keshmarzi, E., Tait, R. N., and Berini, P., "Long-range surface plasmon single-mode laser concepts," *J. Appl. Phys.* 112, 063115 (2012).
[9] Karami Keshmarzi, E., Tait, R. N., and Berini, P., "Single-mode surface plasmon distributed feedback lasers," *Nanoscale*, DOI: 10.1039/C7NR09183D
[10] Krupin, O., Asiri, H., Wang, C., Tait, R. N., Berini, P., "Biosensing using straight long-range surface plasmon waveguides," *Opt. Express* 21, 698-709 (2013).
[11] Khan, A., Krupin, O., Lisicka-Skrzek, E., Berini, P., "Mach-Zehnder refractometric sensor using long-range surface plasmon waveguides," *Appl. Phys. Lett.* 103, 111108 (2013).
[12] Fan, H., Berini, P., "Bulk sensing using a long-range surface-plasmon dual-output Mach-Zehnder interferometer," *J. Lightwave Technol.* 34, 2631-2638 (2016).
[13] Fan, H., Berini, P., "Bulk sensing using a long-range surface-plasmon triple-output Mach-Zehnder interferometer," *J. Opt. Soc. Am. B* 33, 1068-1074 (2016).
[14] Krupin, O. *et al.*, "Long-Range Surface Plasmon-Polariton Waveguide Biosensors for Disease Detection," *J. Lightwave Technol.* 34, 4673-4681 (2016).
[15] Wong, W. R. *et al.*, "Serological diagnosis of dengue infection in blood plasma using long-range surface plasmon waveguides," *Anal. Chem.* 86, 1735-1743 (2014).
[16] Krupin, O. *et al.*, "Detection of leukemia markers using long-range surface plasmon waveguides functionalized with protein G," *Lab on a Chip* 15, 4156-4165 (2015).